Journal of Quantitative Spectroscopy & Radiative Transfer 262 (2021) 107524

Contents lists available at ScienceDirect

Journal of Quantitative Spectroscopy & Radiative Transfer

journal homepage: www.elsevier.com/locate/jqsrt

How much is enough? The convergence of finite sample scattering properties to those of infinite media

Antti Penttilä[a,*], Johannes Markkanen[a,b], Timo Väisänen[a], Jukka Räbinä[a,c], Maxim A. Yurkin[d,e], Karri Muinonen[a,f]

[a] Department Physics, University of Helsinki, Finland
[b] Max Planck Institute for Solar System Research, Göttingen, Germany
[c] Faculty of Information Technology, University of Jyväskylä, Finland
[d] Voevodsky Institute of Chemical Kinetics and Combustion, SB RAS, Novosibirsk, Russia
[e] Novosibirsk State University, Russia
[f] Finnish Geospatial Research Institute FGI, National Land Survey, Kirkkonummi, Finland

ARTICLE INFO

Article history:
Received 16 December 2020
Accepted 14 January 2021
Available online 18 January 2021

Keywords:
Scattering
Particulate random media
Radiative transfer
Maxwell equations

ABSTRACT

We study the scattering properties of a cloud of particles. The particles are spherical, close to the incident wavelength in size, have a high albedo, and are randomly packed to 20% volume density. We show, using both numerically exact methods for solving the Maxwell equations and radiative-transfer-approximation methods, that the scattering properties of the cloud converge after about ten million particles in the system. After that, the backward-scattered properties of the system should estimate the properties of a macroscopic, practically infinite system.

1. Introduction

In August 2016, in conjunction with the Union Radio-Scientifique Internationale (URSI) Commission B International Symposium on Electromagnetic Theory in Espoo, Finland, the Department of Physics at the University of Helsinki organized a workshop titled 'One-Billion-Particle Problem' (OBPP).[1] The leading topic of this workshop was to discuss the current state-of-the-art in methods and implementations for solving electromagnetic absorption, extinction, and scattering problems. Especially, we are interested in the scattering properties of a medium that is macroscopic in size, but constitutes of particles or structures with typical sizes close to the wavelength of light.

The scattering of a macroscopic target consisting of wavelength-scale elements is an open problem in computational electromagnetics. Approximate methods based on radiative transfer (RT) method are computationally feasible for macroscopic media, but the pure RT approximation is not valid with close-packed media [1]. Modified RT approaches for dense media have been studied [see, e.g., 2,3], and there are recent advances in modified RT approaches combining rigorous and approximate elements for higher packing densities [4–7]. Several approaches for solving (numerically) exactly the macroscopic Maxwell equations (MEs) governing the problem exist [see, e.g., 8–10]. However, all these methods share the same caveat — as the size of the target compared to the wavelength increases, the required computational resources, such as the CPU-time and the memory, also increase. The current limit in problem sizes possible to solve with these methods is one of the questions to be answered in this work, but roughly speaking, it is currently around $x = \frac{2\pi r}{\lambda}$ from 150 to 300, where x is the size parameter, r is the radius of the volume-equivalent sphere, and λ is the wavelength.

It is clear that as the computational resources needed by numerically exact solvers of electromagnetic scattering increase faster than $\mathcal{O}(n)$ with n being the number of particles or the scattering volume, there will be still limits in the use of direct ME's solvers for large problems. To be exact, in some methods (as in STMM and DDA, see Section 2.1), there is interaction between the particles that needs to be solved. This interaction is naively $\mathcal{O}(n^2)$, but can be implemented as $\mathcal{O}(n \log n)$ with the help of Fast Fourier Transform (in DDA) or Fast Multipole Method (in STMM methods). In addition, there is the number of iterations m needed for the iterative matrix inversion, making the total computational complexity as $\mathcal{O}(m(n \log n))$, where m depends of n but in a complicated manner. In finite-difference type methods (such as DEC, see Section 2.1), the complexity is $\mathcal{O}(mn)$, again with complicated dependence between n and m.

* Corresponding author.
E-mail address: antti.i.penttila@helsinki.fi (A. Penttilä).

[1] See http://wiki.helsinki.fi/display/PSR/OBPP.

https://doi.org/10.1016/j.jqsrt.2021.107524
0022-4073/

One can try to tackle the computational problems with modern supercomputers with thousands of interlinked central or graphics processing units (CPUs or GPUs), but at some point the overhead of the message passing between the processor cores will surpass the performance gain from adding more cores to the task. Thus, it would be beneficial if the scattering properties of finite particulate media would converge to those of macroscopic, practically infinite case at some size. In this work, we will estimate if there is such convergence and at which point. First, in Section 2 we will define the scattering problem given at the OBPP workshop and introduce the codes that were used to solve it. Second, in Section 3 we will show the workshop results, and finally in Section 4 we will discuss and conclude.

2. The one-billion-particle-problem definition

The definition of the scattering problem was given to the workshop participants beforehand. It stated that:[1]

> Consider one billion spherical particles (radius r) randomly located in a finite, spherical medium (radius R) in free space in an incident electromagnetic plane wave field (wavelength λ, wave number $k = 2\pi/\lambda$). Show the ensemble-averaged 4×4 Mueller scattering matrix interrelating the four Stokes parameters ($\boldsymbol{I} = (I, Q, U, V)$) of the incident field and the scattered field when the size parameter ($x = kr$) and complex refractive index (m) of the individual spherical particles are $x = 1.76$ and $m = 1.50 + i10^{-4}$ and when the volume fraction of the spherical particles in the spherical medium is $v = 20\%$.

Furthermore, it stated that in the (expected) case where the problem could not be solved with one billion particles, one may compute with the maximum number of particles still practical for the method. As the participants started producing their answers, we converged having intermediate results for powers of ten in the number of particles, starting from 10^3. The size parameters for the problem with the number of particles is presented in Table 1, and the illustration of the scattering geometry with 10^3 particles is shown in Fig. 1.

2.1. Scattering codes

We had contributions for the OBPP from the workshop participants, and we also conducted extensive simulations using various different codes ourselves at the workshop host institute. The codes that we used are all published, most of them publicly available, so we introduce them next only shortly. While pushing the limits of these codes did require certain fine tuning, we do not discuss it in details, since the main argument is based on the agreement between different independent codes. In most cases, the codes were run on the computing cluster at CSC — IT Center for Science in Finland.

Table 1
Size parameters for the scattering problem with the number of particles (No.) varying in powers of ten, starting from 1,000 particles. The table shows both the size parameter of the particles ($X_{\text{particles}}$, equivalent-volume-sphere radius), and the size parameter of the sphere that circumscribes the particles (X_{sphere}). The columns a–g indicate the codes that were used to compute the results with the corresponding size parameter. The columns are as a - RT-CB, b - RT-CB-ic, c - R^{2}T^2, d - FaSTMM, e - DEC, f - ADDA, and g - MSTM. Please see Section 2.1 for the description of the codes.

No.	$X_{\text{particles}}$	X_{sphere}	a	b	c	d	e	f	g
10^3	17.6	30.1	x	x	x	x	x	x	x
10^4	37.9	64.8	x	x	x	x	x	x	
10^5	81.7	140	x	x	x	x	x	x	
10^6	176	301	x	x	x		x		
10^7	379	648	x	x					
10^8	817	1397	x	x					
10^9	1760	3010	x	x	x				

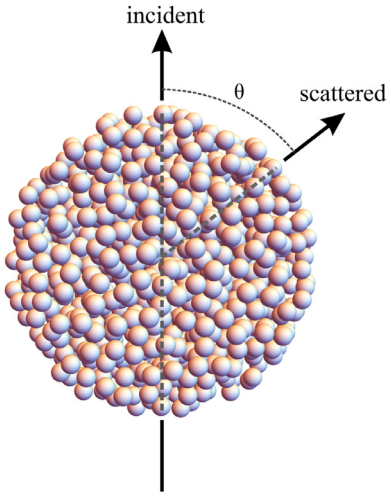

Fig. 1. One random realization of 10^3 equal-sized spheres that are packed in a spherical volume with 20% packing density. The scattering angle θ is the angle between the direction of the incident field and the observing direction of the scattered field.

2.1.1. Numerically exact codes

Superposition T-matrix code MSTM. The MSTM code is developed by Daniel Mackowski, and we used version 3.0 of the code.[2] The code works with perfect spheres and solves the so-called T-matrix of the whole volume as the superposition of all the individual T-matrices from the constituents. The electromagnetic fields are expanded with the spherical vector wave functions (SVWF), and the scatterers in the cluster are represented as the T-matrices, i.e., mappings from the incident SVWF coefficients to the scattered ones. The interactions between the scatterers are computed by employing the translation addition theorems for the SVWF. This yields to the system of linear equations which can be solved numerically. The code is using an MPI-parallelization and can be efficiently used in large computing clusters [11].

Fast superposition T-matrix method FaSTMM. The FaSTMM code is developed by Johannes Markkanen, and formulates the solution to the multiple scattering problem using the field decomposition and the superposition principle.[3] This leads to the so-called superposition T-matrix method (STMM, similarly as with the MSTM code) [12–14].

The FaSTMM uses an iterative solver to solve the linear system in which the matrix-vector multiplication in each iteration step is accelerated with the fast multipole method (FMM) [15]. The FMM decreases the computational complexity of the matrix-vector product from $\mathcal{O}(n^2)$ to $\mathcal{O}(n \log n)$ where n is the number of particles. The FaSTMM is implemented with modern Fortran language and it is parallellized with OpenMP.

Discrete exterior calculus DEC. The DEC code is developed by Jukka Räbinä. The state-of-the-art in finite-difference type techniques is the discrete exterior calculus (DEC), which refers to the intuitive correspondence with its continuous counterpart, i.e., the exterior calculus [16,17]. The cornerstone of DEC is the segregation of differentiable and metric structures. This is to say, the discrete counterparts of the differential operators do not depend on the metric. These so-called "discrete exterior derivatives" fulfill exactly the Stokes theorem. The metric structures (or the material param-

[2] MSTM 3.0, available at http://www.eng.auburn.edu/~dmckwski/scatcodes/.
[3] FaSTMM is available at http://wiki.helsinki.fi/display/PSR/.

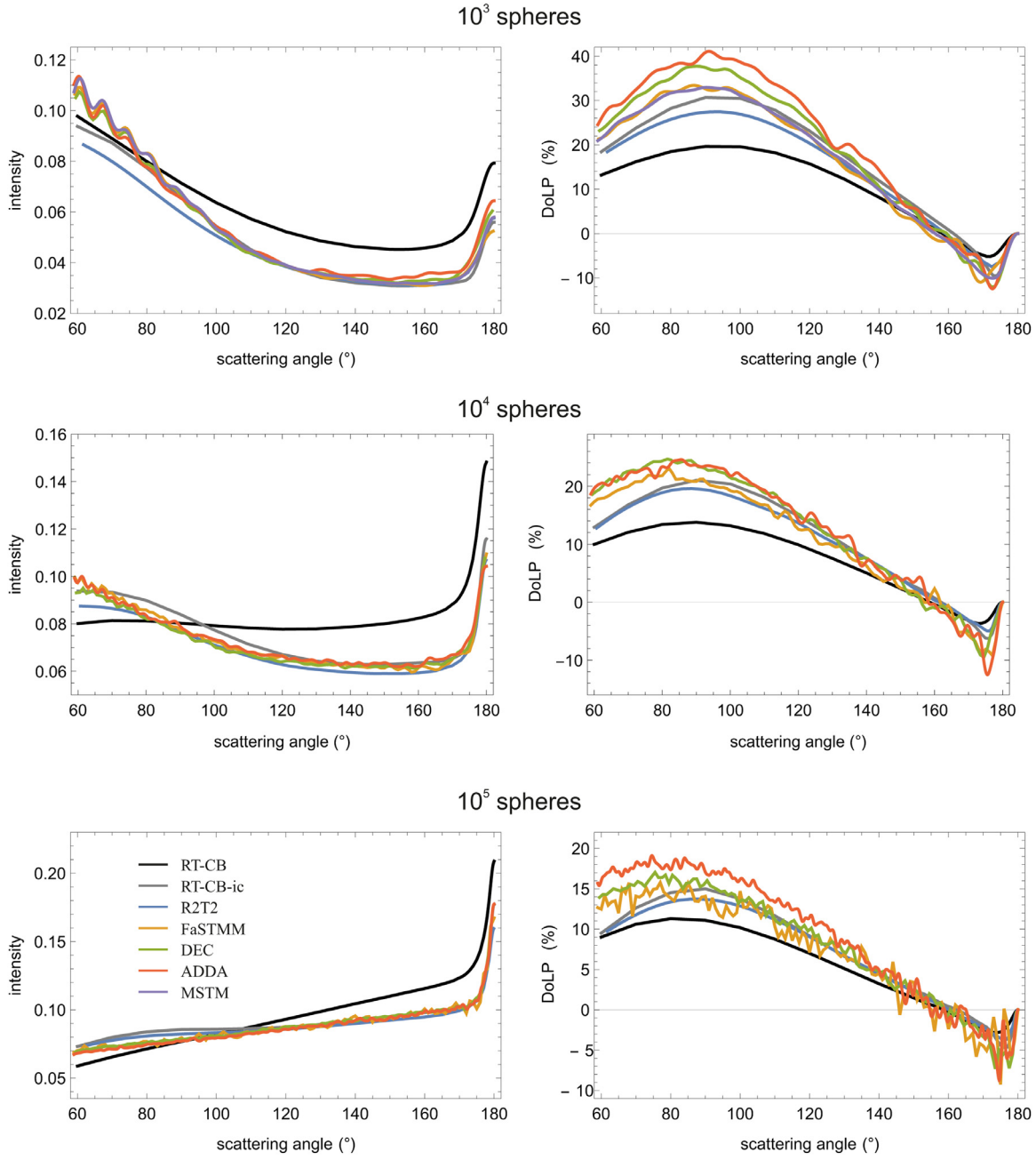

Fig. 2. The intensity and the degree of linear polarization computed with the available codes for the spherical volume containing variable amount of spherical particles in $v = 20\%$ packing density. Continues in Fig. 3.

eters) are approximated with "discrete Hodge" matrices, which are related to geometries of primal and dual meshes.

For efficient implementation of DEC, one should focus on the approximation of the discrete Hodge [18,19]. To minimize the discretization error, a tetrahedral (body-centered cubic) mesh structure has been chosen, which leads to more isotropic wave propagation than with the cubic tiling. Also the discrete Hodge correction, which is based on spatial curvature of the estimated solution, is applied. With these tricks, the numerical wavelength error has been nearly eliminated, which is essential in large problems.

The method is implemented with C++ programming language using message passing interface (MPI) and domain decomposition parallelization.

Discrete dipole approximation code ADDA. The ADDA code is a C99 implementation of the discrete dipole approximation — a method based on the discretization of the volume-integral form of the MEs [20]. ADDA uses an MPI-parallelization for a single-scattering problem and can be efficiently used in large computing clusters [21]. In this manuscript, we are using ADDA version 1.3b4.[4]

The ensemble averaging was replaced by orientation averaging, for which rotation over one Euler angle can be performed at a small computational cost [21]. In other words, for each particle orientation ADDA computed the scattered fields not in a single scattering plane, but rather for a set of planes rotated around the incident direction. More details about ADDA simulations can be found in [22].

[4] ADDA is available at https://github.com/adda-team/adda.

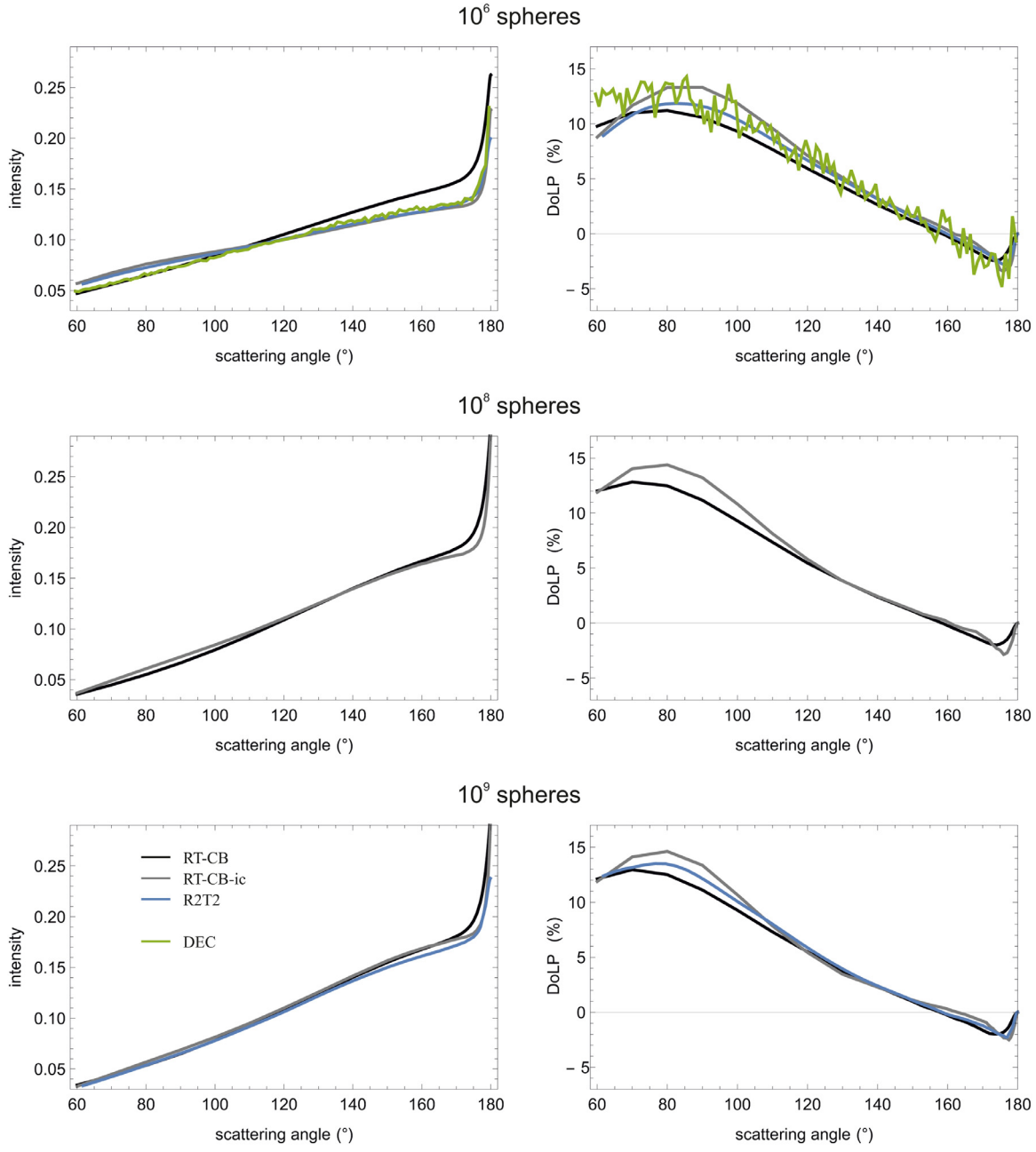

Fig. 3. Continued from Fig. 2.

2.1.2. Radiative-transfer-type approximations

Because the one-billion-particle scattering medium is far too large to be currently solved with the numerically exact codes, we also included three approximate solutions in the comparison. All the approximations are based on the radiative-transfer solution of the electromagnetic scattering, but two of these are modified so that they could better adapt to the non-sparse packing density of $v = 20\%$.

Radiative transfer with coherent backscattering RT-CB. The RT-CB method is developed at the University of Helsinki[5]. It solves the radiative transfer equation (RTE) using Monte Carlo multiple-scattering algorithm. The RTE works well for the sparse medium and hence it is widely used, e.g., in atmosphere modeling. Still, the RTE is oversimplified meaning that it is missing some effects, such as the coherent backscattering (CB). The CB causes the intensity peak and the negative polarization surge in the backscattering angles. The RT-CB traces rays inside the medium and by tracing another ray in reversed order and solving the interference of these rays, a CB effect is added to the RT solution [23].

Radiative transfer and coherent backscattering with incoherent fields RT-CB-ic. The applicability of the RT-CB can be extended to the dense media by using an input generated with the incoherent fields [24]. The input is created by generating a set of volume elements, and computing the first-order incoherent scattering properties from these using them. The generated incoherent Mueller matrix and the mean free path can be then used with the RT-CB.

Radiative transfer with reciprocal transactions R^2T^2. The R^2T^2 method is developed at the University of Helsinki[6] [4,6]. The

[5] RT-CB is available at http://wiki.helsinki.fi/display/PSR/.

[6] R^2T^2 is available at http://wiki.helsinki.fi/display/PSR/.

method employs the T-matrix method to handle the interaction between the electric fields and the incoherent volume element but functions similarly to the RT-CB. The scattering properties of the incoherent volume elements are precomputed with an exact method and transferred to the R^2T^2 using the T-matrices. Due to the T-matrix formalism, the R^2T^2 accepts any volume element that can be presented with the T-matrix [5]. Compared to the RT-CB-ic, the R^2T^2 should produce results that are closer to the exact ones because the way R^2T^2 handles the incoherent volume is more rigorous and does not use averaged properties.

3. Results

With all the codes, the Mueller matrix of the target, as a function of the scattering angle, was computed. In addition, the integrated quantities of scattering and absorption efficiency Q_{sca} and Q_{abs}, which are the scattering and the absorption cross-sections C_{sca} and C_{abs} normalized with the cross-sectional area of the circumscribing sphere, were computed. Please note that the intensity (M_{11}, the (1,1) element of the Mueller matrix) is normalized in all results so that the integration over the unit sphere equals to Q_{sca} of the target:

$$Q_{csa} = \int_0^{2\pi} \int_0^{\pi} \sin(\theta)\, M_{11}(\theta)\, d\theta\, d\phi, \tag{1}$$

Table 1 shows the cases that were computed and the codes that produced results for those cases. The numerically-exact-code computations were pushed to the current practical limits using a modern supercomputer[7], except for the MSTM code. The FaSTMM and the MSTM codes are so similar in their methodology, that the MSTM was only used for 1,000 particles to cross-validate the FaSTMM results.

The intensity and the degree of linear polarization (DoLP) for cases with 10^3, 10^4, 10^5, 10^6, 10^8, and 10^9 spheres are shown in Figs. 2–3. The case with 10^7 spheres is so similar to 10^8 spheres, and only computed with the RT-CB and RT-CB-ic codes that it was left out of the figure. We are showing only the scattering angles starting from 60°, since the forward-scattering angles contain the diffraction with the numerically exact codes but not with the RT-based approximations, and also because we are more interested in the scattering effects by the particles than the volume as whole. All the numerically exact results are averaged over multiple realizations of the particle positions in the media. Owing to the fact that the corresponding computations with large number of particles are very heavy, especially the DoLP values are not that well averaged but contain still some speckle effects from the individual realizations that are not completely averaged out.

From the results shown in Figs. 2-3 we can see that the approximate methods, especially the RT-CB-ic and R^2T^2 that are corrected to be applicable to dense media, start to follow the numerically exact results quite well with 10^5 spheres or more in the volume. The intensity, including the sharp backscattering enhancement, is modeled very well. The DoLP results vary more even within the numerically exact methods, due to the limited number of configuration averages or the different discretized representation of spherical shape in the codes. In any case, the inversion angle of the DoLP from positive to negative, and the shape of the negative polarization lobe that is related to the coherent backscattering, are quite well agreed with all the codes. The location of the polarization maximum might be modeled a bit too far in the scattering angle with the RT-based approximations. This is associated with the lack of accounting the coherent field in the RT approximations, as noted in [25,26].

We were able to run numerically exact simulations with the DEC code using one million particles, which is already quite an impressive result. That result, together with the other numerically exact results with 10^5 particles, seem to indicate that the dense-media-corrected RT codes RT-CB-ic and R^2T^2 are producing results that approximate quite well the true behavior starting from 10^5–10^6 particles. What is interesting is that also the traditional RT method that includes the coherent-backscattering approximation (RT-CB) starts to approach these more accurate RT-CB-ic and R^2T^2 results with 10^7–10^9 spheres. We note that these nice results are here found for quite transparent media with $\mathrm{Im}(m) = 10^{-4}$, and there can be challenges with RT-based methods in highly absorbing material [6].

In addition to the angular intensity and DoLP profiles, and scattering and absorption efficiencies Q_{sca} and Q_{abs}, we have also computed the 'backscattering efficiency' Q_{bcsa} as

$$Q_{bcsa} = \int_0^{2\pi} \int_{\pi/2}^{\pi} \sin(\theta)\, M_{11}(\theta)\, d\theta\, d\phi, \tag{2}$$

where the Mueller matrix is normalized as in Eq. (1).

4. Discussion

One of the long-standing questions in multiple scattering by small particles is that at which size (i.e., number of scatterers, surface area, volume, etc.) our (numerically) exact results converge in the far field. In detail, the quantity we are after could be the shape of the scattering phase function (of some Mueller matrix element), or an integrated property such as the scattering or absorption cross section [27]. If we would be able to accurately simulate a volume that is so large that its scattering properties do not further depend on the volume size, we could generalize them to apply for truly macroscopic targets.

One can assume that the possible convergence to macroscopic sample properties would show up first, or at least with less fluctuations, in the integrated quantities such as the scattering or absorption efficiency. In media infinite in both perpendicular and parallel directions of the incident wave, there is no forward scattering, so we study the behavior of the backscattering efficiency Q_{bsca} defined in Eq. (2), see Fig. 4. As also the angular scattering properties seem to indicate (Figs. 2-3), the dense-media corrected

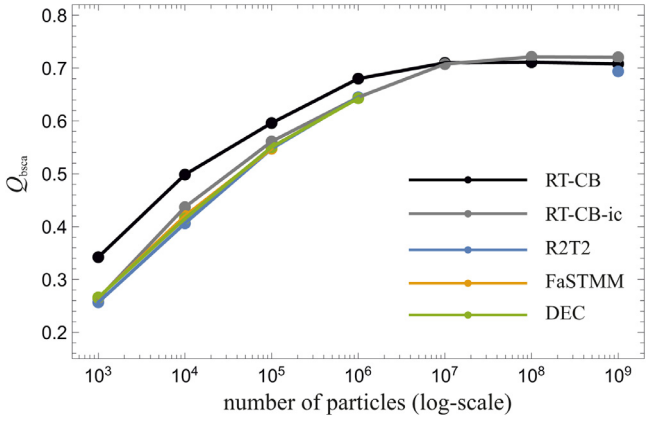

Fig. 4. The backscattering hemisphere scattering efficiency Q_{bcsa} as a function of the target size, expressed as the number of the particles in the cloud. The Q_{bcsa} is shown here for five methods, of which the FaSTMM and DEC rigorously solve the macroscopic Maxwell equations, and the RT-CB, RT-CB-ic, and R^2T^2 are based on the radiative transfer approximation. The results with ADDA go up to 10^5 particles and MSTM to 10^3 particles, they follow the same overall trend but are not shown here.

[7] The Taito supercluster from HP with over 400 Intel Xeon Haswell computing nodes. Each node has two processors, 24 cores, and at least 128 GB of memory per node. The computer is provided by the CSC.

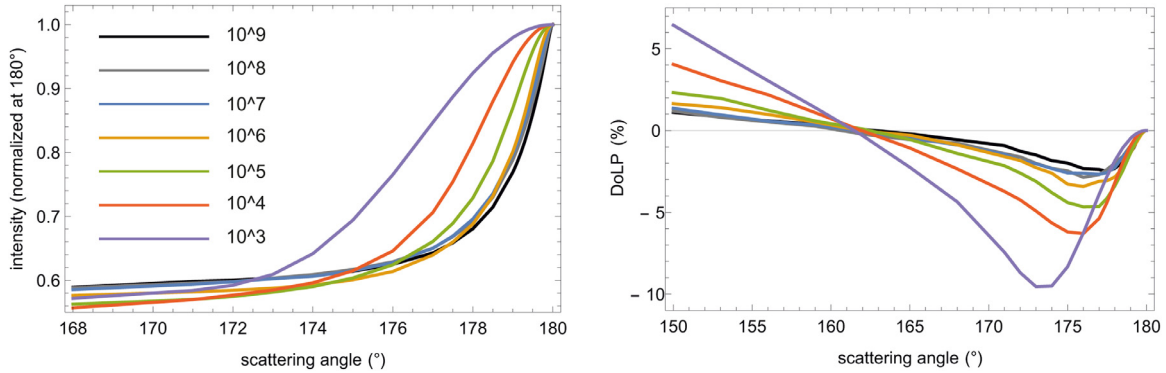

Fig. 5. The scattering phase function (in the left) and the degree of linear polarization (in the right) for backscattering region. Results are computed with the RT-CB-ic method. The plot legend panel indicates the powers of ten for the number of particles in the target.

RT methods agree well with the numerically exact methods. Also, with 10^7 particles or more, the regular RT seems to converge with the corrected ones.

What is extremely interesting, is that starting from 10^7 particles or so, the Q_{bcsa} seems to converge to a constant value of about 0.7. This happens both for the regular RT and for the dense-media-corrected ones. On the other hand, the RT-CB-ic and R^2T^2 values follow loyally the numerically-exact-method values up to the point where the latter can still be used, 10^6 particles. This would suggest that the scattering properties of the target are converging with about 10 million particles (volume-equivalent size parameter of particles about 400, circumscribing sphere size parameter about 650).

The same limit of 10^7 particles seems to hold if we look at the shape of the scattering phase function or the degree of linear polarization close to backscattering (see Fig. 5). Both the shape of the coherent backscattering peak and the negative degree of linear polarization converge after this limit in the RT-CB-ic results. The traditional RT-CB results are very similar (not shown here).

According to the results above, it seems that for this particular problem, the scattering properties of the system start to converge at about 10^7 particles or at the circumscribing volume size parameter of 650. On one hand, this result is unique to this particular scattering target. On the other hand, the individual particles are close to the wavelength size ($x = 1.76$), which means that they are efficient scatterers. Furthermore, there is almost no absorption in the system, the single-scattering albedo of the single sphere in the system is $\varpi = 0.999374$. Thus, one can expect excessive multiple scattering for this system. With less multiple scattering or with smaller single-scattering albedos, the convergence might be achieved earlier. That is why we conclude that a system with 10 million particles with sizes in the wavelength range can be considered to have the scattering properties in the backward-reflected hemisphere of a macroscopic system.

Declaration of Competing Interest

No conflict of interest.

Acknowledgments

We acknowledge the ERC Advanced Grant no. 320773 entitled Scattering and Absorption of Electromagnetic Waves in Particulate Media (SAEMPL). Computational resources were provided by CSC — IT Centre for Science Ltd, Finland. The development of ADDA is supported by the Russian Science Foundation (Grant no. 18-12-00052).

We would like to thank all the workshop participants, Jani Tyynelä, Timo Nousiainen, Jouni Peltoniemi, Daniel Mackowski, Dimitrios Tzarouchis, Xavier Faget, and Fatih Dikmen (list excluding the authors of this article). Special thanks to the Chairman of the Finnish National Committee of URSI, Ari Sihvola for allowing us to organize the workshop as part of the EMTS conference.

References

[1] Mishchenko M, Goldstein D, Chowdhary J, Lompado A. Radiative transfer theory verified by controlled laboratory experiments. Opt Lett 2013;38(18):3522–5. doi:10.1364/OL.38.003522.
[2] Tsang L, Chen C-T, Chang A, Guo J, Ding K-H. Dense media radiative transfer theory based on quasicrystalline approximation with applications to passive microwave remote sensing of snow. Radio Sci 2000;35(3):731–49. doi:10.1029/1999RS002270.
[3] Tishkovets V, Jockers K. Multiple scattering of light by densely packed random media of spherical particles: dense media vector radiative transfer equation. J Quant Spectrosc Radiat Transf 2006;101(1):54–72. doi:10.1016/j.jqsrt.2005.10.001.
[4] Muinonen K, Markkanen J, Väisänen T, Peltoniemi J, Penttilä A. Multiple scattering of light in discrete random media using incoherent interactions. Opt Lett 2018;43(4):683–6. doi:10.1364/OL.43.000683.
[5] Markkanen J, Väisänen T, Penttilä A, Muinonen K. Scattering and absorption in dense discrete random media of irregular particles. Opt Lett 2018;43(12):2925–8. doi:10.1364/OL.43.002925.
[6] Väisänen T, Markkanen J, Penttilä A, Muinonen K. Radiative transfer with reciprocal transactions: numerical method and its implementation. PLoS ONE 2019;14(1):1–24. doi:10.1371/journal.pone.0210155.
[7] Ramezanpour B, Mackowski D. Direct prediction of bidirectional reflectance by dense particulate deposits. J Quant Spectrosc Radiat Transf 2019;224:537–49. doi:10.1016/j.jqsrt.2018.12.012.
[8] Light scattering by nonspherical particles: theory, measurements, and applications. Mishchenko M, Hovenier J, Travis L, editors. Academic Press; 2000.
[9] Mishchenko M. Electromagnetic scattering by particles and particle groups: an introduction. Cambridge University Press; 2014.
[10] Kahnert M. Numerical solutions of the macroscopic Maxwell equations for scattering by non-spherical particles: a tutorial review. J Quant Spectrosc Radiat Transf 2016;178:22–37. doi:10.1016/j.jqsrt.2015.10.029.
[11] Mackowski D, Mishchenko M. A multiple sphere *T*-matrix Fortran code for use on parallel computer clusters. J Quant Spectrosc Radiat Transf 2011;112(13):2182–92. doi:10.1016/j.jqsrt.2011.02.019.
[12] Bruning J, Lo Y. Multiple scattering of EM waves by spheres Part I — multipole expansion and ray-optical solutions. IEEE Trans Antennas and Propag 1971;19(3):378–90. doi:10.1109/TAP.1971.1139944.
[13] Bruning J, Lo Y. Multiple scattering of EM waves by spheres Part II — numerical and experimental results. IEEE Trans Antennas Propag 1971;19(3):391–400. doi:10.1109/TAP.1971.1139925.
[14] Peterson B, Ström S. *T* matrix for electromagnetic scattering from an arbitrary number of scatterers and representations of E(3). Phys Rev D 1973;8:3661–78. doi:10.1103/PhysRevD.8.3661.
[15] Markkanen J, Yuffa A. Fast superposition T-matrix solution for clusters with arbitrarily-shaped constituent particles. J Quant Spectrosc Radiat Transf 2017;189:181–8. doi:10.1016/j.jqsrt.2016.11.004.
[16] Desbrun M, Kanso E, Tong Y. Discrete differential forms for computational modeling. In: Bobenko A, Schröder P, Sullivan J, Ziegler G, editors. Discrete differential geometry, vol. 38 of Oberwolfach seminars. Birkhäuser; 2008. p. 287–324.
[17] Stern A, Tong Y, Desbrun M, Marsden J. Geometric computational electrodynamics with variational integrators and discrete differential forms. In: Chang D, Holm D, Patrick G, Ratiu T, editors. Geometry, mechanics, and dynamics; vol. 73 of Fields institute communications. New York: Springer; 2015. p. 437–75.

[18] Räbinä J. On a numerical solution of the Maxwell equations by discrete exterior calculus. University of Jyväskylä, Finland; 2014. Doctoral thesis. http://urn.fi/URN:ISBN:978-951-39-5951-7.
[19] Räbinä J, Mönkölä S, Rossi T. Efficient time integration of Maxwell's equations with generalized finite differences. SIAM J Sci Comput 2015;37(6):B834–54. doi:10.1137/140988759.
[20] Yurkin M, Hoekstra A. The discrete dipole approximation: an overview and recent developments. J Quant Spectrosc Radiat Transf 2007;106:558–89. doi:10.1016/j.jqsrt.2007.01.034.
[21] Yurkin M, Hoekstra A. The discrete-dipole-approximation code ADDA: capabilities and known limitations. J Quant Spectrosc Radiat Transf 2011;112(13):2234–47. doi:10.1016/j.jqsrt.2011.01.031.
[22] Yurkin M.. Exact solution, capabilities of discrete-dipole approximation code ADDA. 2016. Conference presentation. doi:10.13140/RG.2.2.30352.20489.
[23] Muinonen K. Coherent backscattering of light by complex random media of spherical scatterers: numerical solution. Waves Random Media 2004;14:365–88.
[24] Muinonen K, Markkanen J, Väisänen T, Peltoniemi J, Penttilä A. Multiple scattering in discrete random media using first-order incoherent interactions. Radio Sci 2017;52(11):1419–31. doi:10.1002/2017RS006419.
[25] Markkanen J, Agarwal J, Väisänen T, Penttilä A, Muinonen K. Interpretation of the phase functions measured by the OSIRIS instrument for comet 67P/Churyumov-Gerasimenko. Astrophys J Lett 2018;868(1):L16. doi:10.3847/2041-8213/aaee10.
[26] Muinonen K, Väisänen T, Martikainen J, Markkanen J, Penttilä A, Gritsevich M, et al. Scattering and absorption of light in planetary regoliths. J Vis Exp 2019;149:e59607. doi:10.3791/59607.
[27] Videen G, Muinonen K. Light-scattering evolution from particles to regolith. J Quant Spectrosc Radiat Transf 2015;150:87–94. doi:10.1016/j.jqsrt.2014.05.019.